Biochimica et Biophysica Acta, 1063 (1991) 179–190

ADONIS 000527369100150G

BBAMEM 75156

Transport parameters in the human red cell membrane: solute-membrane interactions of amides and ureas

Michael R. Toon and A.K. Solomon

Biophysical Laboratory, Harvard Medical School, Boston, MA (U.S.A.)

(Received 26 September 1990)

Key words: Erythrocyte membrane; Permeability; Water; Amide; Urea; Reflection coefficient

We have studied the permeability of a series of hydrophilic amides and ureas through the red cell membrane by determining the three phenomenological coefficients which describe solute–membrane interaction: the hydraulic permeability (L_p), the phenomenological permeability coefficient (ω_i) and the reflection coefficient (σ_i). In 55 experiments on nine solutes, we have determined that the reflection coefficient (after a small correction for solute permeation by membrane dissolution) is significantly less than 1.0 ($P < 0.003$, t-test), which provides very strong evidence that solute and water fluxes are coupled as they cross the red cell membrane. It is proposed that the aqueous channel is a tripartite assembly, comprising H-bond exchange regions at both faces of the membrane, joined by a narrower sieve-specific region which crosses the lipid. The solutes bind to the H-bond exchange regions to exchange their solvation shell with the H-bonds of the channel; the existence of these regions is confirmed by the finding that the permeation of all the amides and ureas requires binding to well-characterized sites with K_m values of 0.1–0.5 M. The sieve-specific regions provide the steric restraints which govern the passage of the solutes according to their size; their existence is shown by the findings that: (1) the reflection coefficient (actually the function [1 − corrected σ_i]) is linearly dependent upon the solute molecular diameter; and (2) the permeability coefficient is linearly dependent upon solute molar volume. These several observations, taken together, provide strong arguments which lead to the conclusion that the amides and urea cross the red cell membrane in an aqueous pore.

Introduction

The interaction of a membrane with a permeating solute, i, can be described by three phenomenological coefficients: the hydraulic permeability (L_p), the permeability coefficient (ω_i) and the reflection coefficient (σ_i) following the equations given by Katchalsky and Curran [1]. We have previously devised a technique to determine all three of these coefficients in a single series of experiments (Toon and Solomon [2]) and have used this technique to study the interactions of the short-chain aliphatic alkanols with the red cell membrane. We have now extended these studies to another class of solutes, the short chain hydrophilic amides and ureas, which bind to the red cell membrane with much greater specificity than do the alkanols.

Correspondence: A.K. Solomon, Biophysical Laboratory, Harvard Medical School, Boston MA02115, U.S.A.

These studies lead to important conclusions about the permeation of amides through red cell membranes. By applying a small correction for transport by dissolution in the membrane, the reflection coefficient is transformed (using Eqn. 6) into $f(\sigma_i)$, a function which describes the coupling between solute and solvent in the aqueous channel. We find that $f(\sigma_i)$ is linearly dependent upon solute diameter and is significantly greater than zero for all the hydrophilic solutes whose diameter is smaller than that of the equivalent pore. These observations provide strong physical-chemical and thermodynamic evidence of coupling between solute and water flux in passage across the red cell membrane. As solute diameter rises, solute permeability falls, which we ascribe to steric hindrance within the aqueous channel. Consistent with these correlations, we find that $f(\sigma_i)$ is also linearly dependent upon the solute permeability coefficient which shows that, the easier it is for these solutes to permeate the membrane, the less is the osmotic pressure they develop.

Materials and Methods

Materials

All amides and substituted ureas were obtained from Aldrich Chemical Co. (Milwaukee, WI); Bis-Tris propane (1,3-bis[tris(hydroxymethyl)methylamino]propane) from Sigma (St. Louis, MO); and urea from Fisher Scientific (Fairlawn, NJ). All chemicals were of reagent grade. Outdated bank blood was kindly supplied by the Children's Hospital (Boston, MA).

Methods

Outdated bank blood, after aspiration of plasma and buffy coat, was washed three times with a buffer (stopped-flow buffer) of the following composition, in mM: NaCl, 142; KCl, 4.4; $MgCl_2$, 0.5; $CaCl_2$, 1.2; Bis-Tris propane, 20; pH 7.4; 300 ± 5 mosM. Osmolalities of all solutions were determined with a Fiske Model OS osmometer (Uxbridge, MA). Cells at 2% hematocrit were mixed with an equal volume of buffer made hyperosmolal by the addition of NaCl or permeant solute and the time course of red cell volume changes was measured by 90° scattered light using the stopped-flow apparatus of Terwilliger and Solomon [3]. Each numbered experiment was done with a different sample of blood. The analog data were digitized and averaged by a Hewlett-Packard Model 217 computer which was also used for the data analysis. Experiments were carried out at 21–23° C.

Measurement of reflection coefficient

The reflection coefficients, σ_i, reported in this paper were determined by the zero-time method of Goldstein and Solomon [4] as modified by Chasan and Solomon [5]. This method is based on the Kedem-Katchalsky equation (see Ref. 1) for volume flow, J_v ($cm^3\ cm^{-2}\ s^{-1}$):

$$J_v = -L_p\Delta\pi_{imp} - \sigma_i L_p \Delta\pi_{perm} \quad (1)$$

in which the subscripts imp and perm represent impermeable and permeable solutes, L_p is the hydraulic conductivity ($cm^3 dyn^{-1} s^{-1}$) and $\Delta\pi$ is the osmotic pressure difference across the membrane (osmol cm^{-3}). One set of experiments is carried out in which $\Delta\pi_{imp}$ is varied, holding $\Delta\pi_{perm} = 0$, so that L_p can be determined (in light scattering units) from the slope of J_v against $\Delta\pi_{imp}$. Since the internal volume and solute concentration are known analytically only at $t = 0$, J_v is measured at $t = 0$ by extrapolation of the initial time points. A second analogous set of experiments is carried out to determine $\sigma_i L_p$ (in light scattering units) by varying $\Delta\pi_{perm}$, holding $\Delta\pi_{imp} = 0$. σ_i is then determined directly from the ratio of the slopes. The experiments were carried out and the determinations were made as described in detail by Toon and Solomon (Ref. 6 and subsequently, Ref. 2).

Briefly, the time course of 90° light scattering (which is proportional to cell volume) was recorded and digitized, and the results for a series of 25 duplicate runs were averaged over a period from 8 to about 300 ms. After subtraction of the average of 25 control runs (in which cells are mixed with the buffer in which they are suspended, so there is no change in cell volume), the data were fitted by non-linear least squares to a third-order polynomial. The zero-time rate of volume change, the slope at $t = 0$, is given by the coefficient of the linear term in the polynomial, and a typical fit for the averaged urea light scattering data to the fitted polynomial is shown in Fig. 1A. The effects of delays due to dead-time, the unstirred layer and the time at which the initial point is sampled are discussed in detail by Toon and Solomon [6], who conclude that the resultant net correction of $5 \pm 3\%$ is small enough to be neglected. Fig. 1B shows that the initial slope depends linearly on the osmotic pressure gradient for both permeable and impermeable solutes, according to Eqn. 1, for a typical urea experiment.

In the experiments to determine the permeability coefficient, ω_i, we also needed to determine L_p, as discussed in the next section. For this purpose we fitted the entire time course of the cell shrinking curve to Eqn. 3, as discussed below, so that it is possible to compare the values of the initial slope determined by the zero-time measurement of cell volume change with the values of L_p determined from the fit to the exact equation. Fig. 1C shows the correlation in an experiment from the urea series using data obtained over the gradient range of 150 to 373 mosmolal NaCl. The fit is excellent, with the correlation coefficient, $r = 0.998$.

Measurement of permeability coefficient

The permeability coefficients, ω_i, were determined by the minimum method of Sha'afi et al. [7]. In these experiments, cells in isosmotic buffer are mixed with the same buffer to which a permeant solute is added. Under these conditions the cells first shrink to a minimum volume and then swell again to their final volume when both the activity gradients of the permeant solute and of the water have fallen to zero. ω_i is determined from the second derivative of the rate of volume change at the minimum volume, $(d^2V'/dt^2)_{min}$, together with the ratio of the minimum volume to the original volume, according to the equations given in Sha'afi et al. [7]:

$$\omega_i = V'_{min}(d^2V'/dt^2)_{min}/A^2 L_p RT\left(\pi^{o}_{imp} - \pi^{\Delta x}_{imp}\right) \quad (2)$$

in which V' is the volume of cell water, V'_{min} refers to minimum volume and π_{imp} is the osmotic pressure of the impermeant solute at the outside of the cell (superscript, o) or inside (Δx). A is the red cell area, taken as

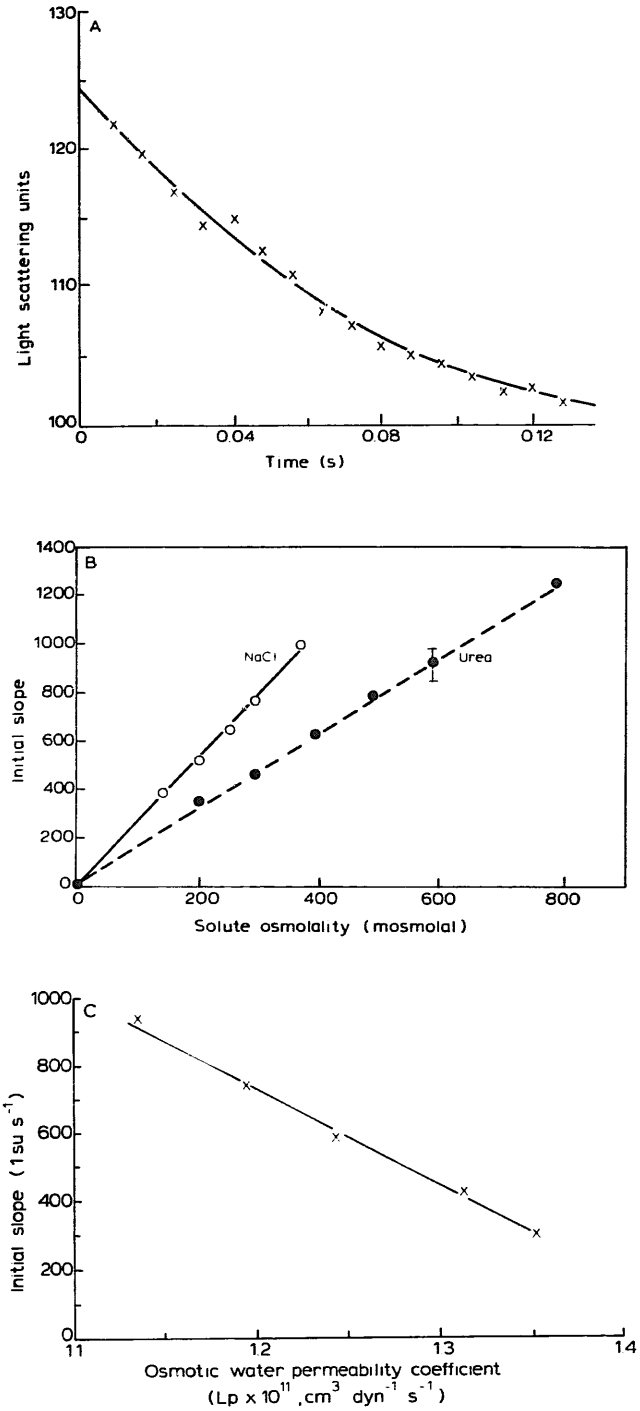

Fig. 1. (A) Red cell volume measured in light scattering units (lsu) as a function of time in an experiment with 400 mmolal urea, as used for the determination of σ_i by the zero-time method of Chasan and Solomon. The data have been fit by non-linear least squares to a second order polynomial with $a_1 = 124$ lsu, $a_2 = -311$ lsus^{-1} and $a_3 = 2122$ lsus^{-2}. (B) The initial slope of red cell volume change (lsus^{-1}) as a function of external osmotic pressure (mosmolal). The error bars are contained within the points for every data set except for the one at 600 mosmolal urea. (C) Comparison of the initial slope method for determining σ_i with the analytical solution of the L_p equation. In these experiments which covered the osmolality gradient range from 150 to 373 mosmolal NaCl, $\Delta\pi_{perm} = 0$ and the initial slope is proportional to L_p according to Eqn. 1. These initial slope values correlate very well ($r = 0.998$) with the values of L_p determined from the fit of the data to the exact equation (in a companion experiment) to the entire time course of cell volume change.

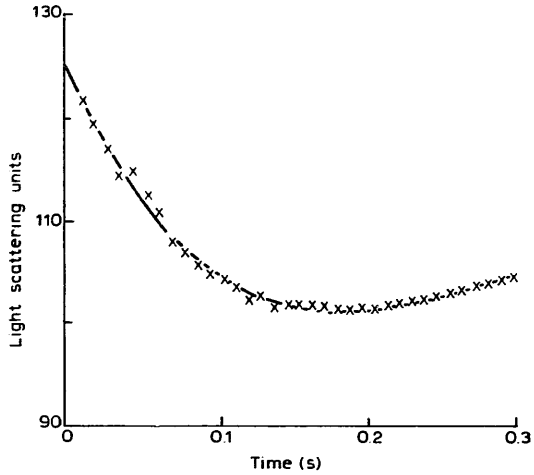

Fig. 2. Red cell volume measured in light scattering units (lsu) as a function of time in an experiment with 400 mmolal urea, as used for the determination of ω_i by the minimum volume method. The data have been fitted by non-linear least squares to a third-order polynomial with $a_1 = 124$ lsu, $a_2 = -314$ lsus^{-1}, $a_3 = 1318$ lsus^{-2} and $a_4 = -1626$ lsus^{-3}.

$1.35 \cdot 10^{-6}$ cm^2, following Jay [8], and R and T have their usual meanings. The data are fitted by non-linear least squares to a third-order polynomial over the range from zero-time to just past the minimum volume and $(d^2V'/dt^2)_{min}$ is obtained from the slope at the minimum volume. The fits are very good, as shown by the typical fit to ethylene glycol data, shown as Fig. 1A in the preceding article in this series [2]. The ethylene glycol data were fitted to an average of 25 runs, whereas 30–40 runs were averaged for the most permeant solutes in this paper.

Computation of ω_i by Eqn. 2 also requires knowledge of the fractional cell water content, 0.71 under

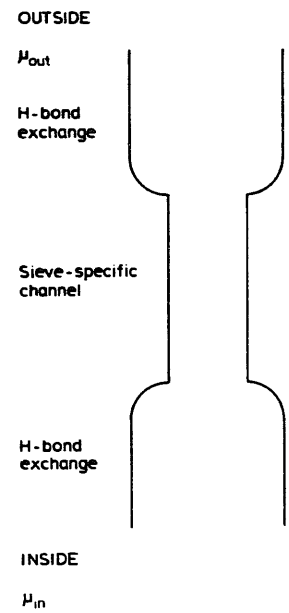

Fig. 3. Schematic drawing of red cell equivalent pore. The chemical potentials of water and solute in the inside and outside solutions are denoted schematically as μ_{in} and μ_{out}.

isosmolal conditions (Savitz et al. [9]), the fraction of non-osmotic water, taken as 0.43 (see Solomon et al. [10]) as well as the value of L_p, which varies from blood to blood. Therefore, for each ω_i measurement, L_p was determined at the same time in cells under essentially identical conditions by fitting the data for the entire time course to the following equation, following Levin et al. (Ref. 11, their equation 3), as corrected by Solomon [12]:

$$L_p = \frac{V_{c,iso}}{ART(\pi^o)^2 t}\pi^i_{iso}[1-(V_b/V_{c,iso})] \times\left[\ln\frac{\pi^i_{iso}-\pi^o}{\pi^i_{iso}-Q\pi^o} - \frac{\pi^o[(V_c/V_{c,iso})-1]}{\pi^i_{iso}(1-(V_b/V_{c,iso}))}\right] \quad (3)$$

In this notation, the superscript, i, refers to the inside of the cell. The subscript, iso, refers to isosmolar conditions. V_b is the apparent non-osmotic water plus cell solutes and membrane volume, as determined from a plot of cell volume (V_c) as function of medium osmolality, which follows the equation:

$$\hat{V}_c = (1-\hat{V}_b)\pi^i_{iso}/\pi^i + \hat{V}_b \quad (4)$$

Volumes have been normalized so that $\hat{V}_c = V_c/V_{c,iso}$ and $\hat{V}_b = V_b/V_{c,iso}$.

$$Q = [(\hat{V}_c - \hat{V}_b)/(1-\hat{V}_b)] \quad (5)$$

The averaged data from a series of thirty consecutive runs was fit to Eqn. 3 by the non-linear least-squares program for L_p written by Dix (private communication) which gives us not only L_p but also the factor which converts light scattering units to cell volume units.

The next step is to feed these values into the non-linear least-squares program for ω_i written by Dix and Levin (private communication). This is the program which fits the averaged light scattering data to the third-order polynomial, determines its minimum and provides the computed value of ω_i. Fig. 2 shows an example of the fit of the curve computed by the ω_i program to the experimental data in a typical urea experiment.

The difference between thermodynamic units of permeability and practical units arises because the thermodynamic driving force is μ_i and the practical unit is c_i. To a first approximation, $\mu_i \approx RTc_i$ so that the major component of the conversion is RT. The practical unit of filtration, P_f (cm s^{-1}) $= RTL_p/\bar{V}$ and the conversion factor $RT/\bar{V} = 1.34 \cdot 10^9$ dyn cm^{-2} at 20 °C. The practical unit of permeability, P_d (cm s^{-1}) $= \omega RT$ and the conversion factor, $RT = 2.44 \cdot 10^{10}$ dyn cm mol^{-1} at 21 °C.

Concentration dependence of ω

It has long been known (Mayrand and Levitt [13]; Wieth et al. [14]) that urea permeability saturates at high concentrations, as Fig. 5 also shows, which means that ω depends upon solute concentration and is not a constant. The Kedem-Katchalsky equations which define ω are derived from a set of phenomenological equations which relate the fluxes in the system to the driving force, in this case the difference in chemical potentials of solute and solvent between outside and inside solutions, denoted schematically in Fig. 3 as μ_{out} and μ_{in}. The coefficients which relate the flows to the driving forces are phenomenological coefficients which need not be constants and may, specifically, be functions of solute concentration, which is not the case for rate constants in conventional chemical reactions. Consequently ω, which is derived from the phenomenological coefficients (see Ref. 1), can (and does) depend upon solute concentration without affecting the validity of the Kedem-Katchalsky equations, from which the Sha'afi et al. method [7] for determining ω has been derived.

According to our present view, the permeation process for urea and most of the solutes we have studied comprises three steps, as proposed by Toon and Solomon [2] and discussed in the next section of this paper: (i) exchange of the solute hydration shell with membrane H-bonds, (ii) diffusion through a sieve-specific channel in the membrane, followed by (iii) exchange of membrane H-bonds for the solute hydration shell on the inside of the membrane, as shown schematically in Fig. 3. Yousef and Macey's [15] finding that urea permeation obeys 'simple pore kinetics' is consistent with this model. It can be shown that the H-bond exchange step is very fast by computing the time it takes for a urea molecule to traverse a single channel. The maximum urea flux in our experiments is $4.3 \cdot 10^{-7}$ mol cm^{-2} s^{-1} (computed from Table II). On the basis of a cell area of $1.35 \cdot 10^{-6}$ cm^2/cell [8] and a urea channel density of $0.6 \cdot 10^5$ channels/cell (footnote 1, Ref. 16), $5.8 \cdot 10^6$ urea molecules cross each channel per second, a transit time of $2 \cdot 10^{-7}$ s, fast compared to our observed urea fluxes which are measured in the millisecond range. Thus the H-bond exchange reactions remain essentially at equilibrium during the transport of urea into the cell.

In practice, we measure ω at a number of solute concentrations covering the range of 0.2 to 0.6 M (0.8 M for urea) and fit the data by non-linear least squares to a single site binding curve, from which we obtain the maximum flux and K_m, according to the equation, $\omega = J_{max}/(K_m + [S])$, in which J is flux (mol^2 dyn^{-1} s^{-1} cm^{-3}) and [S] is solute concentration (mol cm^{-3}). J is obtained by multiplying ω, computed as described above, by the extracellular solute concentration, which remains constant during each experimental run. In practical units (mol cm^{-2} s^{-1}), $J = P_d[S]$. We have adopted the convention that ω_i is the permeability

coefficient at K_m (ω_i = maximum flux/$2K_m$) for the values given in Table II. This convention sets the permeability coefficient at the K_m concentration and makes it comparable to the permeability coefficients for solutes in which saturation is not observed. Typically, we traverse the concentration range in four experiments on separate bloods and report the average of four separate fits.

Results and Discussion

Model of red cell water transport channel

Amides have the capacity of forming four H-bonds, since the amine protons can serve as donors and the carbonyl oxygen can serve as an acceptor for two protons. In this respect they differ markedly from the alkanols because each hydroxyl can only serve as the donor of a single proton. The capacity to form H-bonds is reflected in high crystalline densities; urea, which can form six H-bonds, has a density of 1.323. Steric considerations are important in H-bond formation, as illustrated by comparing 1,1-dimethylurea with its density of 1.255 to 1,3-dimethylurea with its density of 1.142. Even more striking, the melting point of 1,1-dimethylurea is 182°C, as compared with 108°C for 1,3-dimethylurea.

When urea is hydrated with a single shell of water molecules, the crystalline molar radius of 2.6 Å is increased to 5.6 Å, which means that hydrated urea would experience great difficulty in permeating the 6.5 Å radius equivalent red cell pore (see discussion in Ref. 6). We have therefore proposed (Toon and Solomon [2]) that it is necessary for urea to exchange its hydration shell in H-bond exchange regions, at the entrance and exit to the pore, and that this exchange accounts for the saturable nature [13,17–18] of urea flux. A similar exchange is required for the amides with their large H-bonding capacity, whereas the permeation of alkanols, with their smaller H-bonding capacity, does not show saturation, except for ethylene glycol and glycerol [2,13]. According to our model of the red cell water channel in Fig. 3, the entrance and exit H-bond exchange regions are larger in diameter than the sieve-specific aqueous channel which crosses the lipid bilayer with an equivalent radius of ≈ 6.5 Å and provides the steric hindrance which is so important a feature in nonelectrolyte permeation. It is very suggestive that the tripartite arrangement of regions in the acetylcholine receptor protein, which have been determined by three-dimensional image reconstruction by Toyoshima and Unwin [19], consists of a pore with external funnels at the inner and outer membrane faces connected by a narrow tube across the bilayer, entirely consistent with the structure we propose for the red cell aqueous channel.

Since the H-bond-specific and the sieve-specific regions of the channel are spatially separate, it is possible for them to be under separate genetic control, or even in separate proteins bound together in a transport protein complex. Thus, genetically induced changes in urea transport, as in the Jk(a-b-) red cells studied by Edwards-Moulds and Kasschau [20] and Fröhlich et al. [21], need not be coupled to other transport properties of the channel.

Determination of σ_i

The most important phenomenological coefficient in providing information about the channel through which solutes enter the cell is σ_i, which varies between the bounds of 0 and 1. As Katchalsky and Curran [1] have discussed, the following equation is satisfied if the solute and solvent traverse the membrane by independent routes.

$$f(\sigma_i) = 1 - (\omega_i \bar{V}_s / L_p) - \sigma_i = 0 \quad (6)$$

in which $\bar{V}_s$ is the partial molar volume of the solute. Table I gives the values of σ_i which we have determined in 59 measurements of ten hydrophilic urea and amide molecules. The irreversible thermodynamic demonstration that solvent and solute flux are coupled by passage through the same channel is given by showing $f(\sigma_i)$ to be significantly different from 0; the P values in the last column show that the differences are significant for nine of these solutes at the 0.003 level or better (t-test). σ_i is 0.94 for the tenth solute, 1,1-dimethylurea, which has the largest diameter of any of the solutes we have studied. This value of σ_i is consistent with the very slow permeation of 1,1-dimethylurea, which can barely squeeze through the channel, and provides a direct demonstration that $f(\sigma_i)$ approaches zero as the molecular diameter approaches the equivalent pore diameter. The significant differences between the values of $f(\sigma_i)$ and zero for these other nine solutes provide strong thermodynamic evidence that these urea and amide molecules cross the rate determining barrier in the red cell membrane through an aqueous channel, consistent with our previous demonstration that the same conclusion holds for the small hydrophilic alcohols [2].

Although the thermodynamic evidence shows that there is coupling between urea and water flux, it does not specify that all of the water channels are also urea channels. However, it is clear that the number of urea channels must be a substantial fraction of the total number of water channels, since σ_i is the coupling coefficient between solute flux and L_p, the hydraulic conductivity which measures the entire aqueous flux. If only a small fraction of the water channels were coupled to solute flow, σ_i would be small compared to 1; Table I shows that $\sigma_{urea} = 0.63$, consistent with coupling in a large fraction of the water channels. The urea permeability coefficient is so large that there must be a large number of urea channels. Toon and Solomon

(footnote 1, Ref. 16) have calculated that there are approx. $0.6 \cdot 10^5$ urea channels/red cell, compared to approx. $1.3 \cdot 10^5$ water channels/red cell, which provides further evidence that urea transport would require a substantial fraction of the water channels. Furthermore, Toon and Solomon [2] recently found that the reagent, BS[3] (bis(succinimidyl suberate)), modulates both ω_{urea} and L_p and showed that ω_{urea} was linearly dependent on L_p. Though none of these experiments exclude the possibility that a small fraction of the water channels are not accessible to urea, they indicate that a very large fraction of the channels are common to urea and water.

Another consequence of the coupling between solute and solvent flux is the existence of solvent drag (see Ref. 1), the flow of solute through the aqueous channel that must accompany a large induced water flow. Brahm and Galey [22] looked for solvent drag effects on urea diffusion across the human red cell by measuring tracer urea efflux when large water fluxes were induced by imposed gradients of 100–150 mM KCl. They first studied the effect of these osmotic flows on tracer water efflux to which it should be linearly related as shown by Andersen and Ussing [23] in toad skin and discussed in the Appendix. Although there is evidence for such a relationship when the tracer water effluxes in Brahm and Galey's Table IIIA are plotted against the osmotic pressure difference (see Fig. A-1 in the Appendix), the correlation is not significant since the correlation coefficient, $r = 0.36$ and $P > 0.1$. To demonstrate that there is no solvent drag on urea tracer flux, it is necessary to show that the solvent drag on water tracer efflux is greater than that on urea tracer efflux. A detailed statistical comparison of the Brahm and Galey data (see Appendix) shows that the probability that the solvent drag effect on water tracer flux (in the four coupled experiments in their Table IIIA) is greater than that on urea tracer flux (in the four coupled experiments at 38 °C in their Table V) is only $P > 0.4$ (t-test). Thus, there is no statistically significant evidence of any difference between the effect of solvent drag on water tracer efflux and that on urea tracer efflux. These are very difficult experiments and they were carefully done; the equivocal nature of the findings is a reflection of just how great the difficulty is.

Our present value of σ_{urea} of 0.63 ± 0.03 agrees remarkably well with our recent determinations [6] of 0.65 ± 0.03 in six experiments and the value of 0.70 ± 0.02 obtained by Chasan and Solomon [5] in five experiments. It is particularly gratifying that the present value confirms the original determination of 0.62 ± 0.02 made thirty years ago by the more primitive methods available to Goldstein and Solomon [4], as do also the values for three other solutes measured in both sets of experiments (see footnote on p. 185).

Goldstein and Solomon [4] measured σ for nine hydrophilic nonelectrolytes and showed that the relation of σ to molecular dimensions fitted the following equation, based on the restricted diffusion equation of Renkin [27]:

$$1-\sigma_i = \{[2(1-a/r)^2-(1-a/r)^4] \times [1-2.104a/r+2.09(a/r)^3-0.95(a/r)^5]\} \times \{[2(1-a_w/r)^2-(1-a_w/r)^4] \times [1-2.104a_w/r+2.09(a_w/r)^3-0.95(a_w/r)^5]\}^{-1} \quad (7)$$

in which a is the radius of the solute, a_w that of water and r is the equivalent pore radius. It has been known for thirty years that the dominant dimension governing

TABLE I

Reflection coefficient for amides and ureas [a]

	Diam (Å)	$\bar{V}_s$ ($cm^3\ mol^{-1}$)	$(\omega \bar{V}_s/L_p)$	σ_i	$f(\sigma_i)$	P [b]
Formamide	4.32	38.6	0.075	0.45 ± 0.08 (4)	0.48 ± 0.07	0.003
N-Methylformamide	4.68	58.4	0.102	0.53 ± 0.08 (4)	0.37 ± 0.06	0.003
Acetamide	5.24	55.4	0.038	0.64 ± 0.06 (9)	0.32 ± 0.06	0.001
N-Methylacetamide	5.32	76.4	0.035	0.72 ± 0.03 (4)	0.25 ± 0.03	0.001
Propionamide	5.20	71.3	0.036	0.72 ± 0.06 (7)	0.24 ± 0.06	0.001
Urea	5.24	44.2	0.099	0.63 ± 0.03 (8)	0.27 ± 0.04	0.001
Methylurea	5.24	62.0	0.034	0.79 ± 0.06 (9)	0.17 ± 0.06	0.001
Ethylurea	5.24	73.4	0.005	0.85 ± 0.02 (6)	0.15 ± 0.02	0.001
1,3-Dimethylurea	5.24	77.2	0.014	0.81 ± 0.03 (4)	0.18 ± 0.03	0.003
1,1-Dimethylurea	5.64	70.2	0.007	0.94 ± 0.04 (4)	0.06 ± 0.04	0.1

[a] Number of experiments (each on a different blood) in parentheses. Errors are S.D. of the mean and S.E. values are lower by a factor of 1/2 to 1/3.

[b] P is the probability that $f(\sigma_i) = 0$, determined by the t-test.

passage of a solute through the red cell pore is the diameter perpendicular to the cylindrical axis, as first demonstrated for passage of dicarboxylic acids into beef erythrocytes by Giebel and Passow [28]. Subsequently, Soll [29] made a careful investigation of the dependence of Eqn. 7 on molecular dimensions, using the nine values of σ_i determined by Goldstein and Solomon [4] and showed that there was a significant correlation between $\log(1-\sigma_i)$ and solute diameter, but not length,

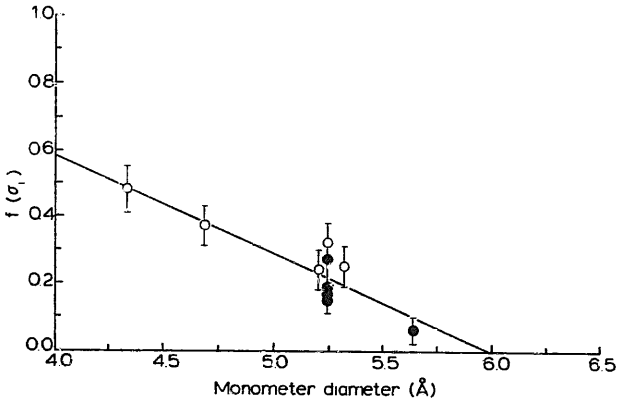

Fig. 4. Dependence of $f(\sigma_i)$ on solute diameter, measured on CPK models. The line through the points was drawn by least squares and has an intercept of 1.75 ± 0.27 and a slope of -0.29 ± 0.05 Å^{-1}. Filled circles denote urea and substituted ureas. The correlation coefficient is 0.83 which is significant at $P < 0.01$ (t-test).

which indicated that the solutes were oriented lengthwise as they traversed the aqueous channel in the membrane. Our data also show that $f(\sigma_i)$ is linearly correlated with the cylindrical diameter of the solute, as shown in Fig. 4. The correlation coefficient is 0.83, which is significant at $P < 0.01$ (t-test) and confirms the conclusion that Soll had reached using our earlier data on a different set of solutes (there are four overlaps, as shown in the footnote *). This correlation argues powerfully that steric restraint within an aqueous channel is a dominant feature governing passage of small hydrophilic solutes across the human red cell membrane.

Determination of ω_i

Well defined low-affinity binding sites, such as those shown in Fig. 5 for urea (mean $K_m = 0.3 \pm 0.07$ molal) and acetamide (mean $K_m = 0.37 \pm 0.15$ molal), are a

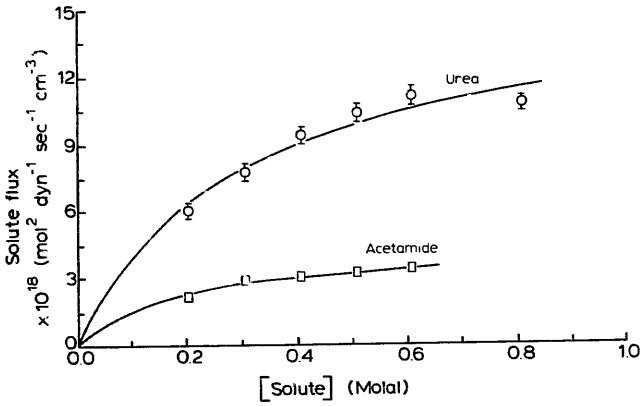

Fig. 5. Dependence of solute flux on concentration in one experiment, typical of seven for urea and three for acetamide. The curves have been fitted to a single site binding curve by non-linear least squares. For urea, $K_m = 0.30 \pm 0.08$ molal and max flux $= (15.8 \pm 1.6) \cdot 10^{-18}$ mol^{2}dyn^{-1}cm^{-3}s^{-1}. For acetamide, $K_m = 0.19 \pm 0.03$ molal and max flux $= (4.5 \pm 0.3) \cdot 10^{-18}$ mol^{2}dyn^{-1}cm^{-3}s^{-1}.

* The following table gives a comparison of the values for σ_i and ω_i in the present paper with those obtained previously by Goldstein and Solomon [4] and Sha'afi et al. [24].

TABLE

Comparison of data for σ_i and ω_i

	σ_i		$\omega_i(10^{-15}$ mol dyn^{-1}s^{-1})	
	this paper	Goldstein and Solomon [4]	this paper	Sha'afi et al. [24] [a]
Formamide	–	–	28.9±9.0	28.8±1.6
acetamide	0.64±0.06	0.58±0.03	11.3±2.2	8.0±0.8
Propionamide	0.72±0.06	0.80±0.03	6.7±1.6	6.4±0.8
Urea	0.63±0.03	0.62±0.02	29.5±7.6	24.0±1.6
Methylurea	0.79±0.06	0.80±0.02	7.6±2.4	3.2±0.5
1,3-Dimethyl-urea	–	–	2.4±0.2	1.8±0.3

[a] Multiplied by 1.6 to compensate for differences in measured red cell area, as discussed in the text.

In 1987, Toon and Solomon [6] also measured σ_i for urea and some substituted ureas and compared their value of $\sigma_{urea} = 0.65 \pm 0.03$ with those in the literature. Our previous values [6] for $\sigma_{methylurea} = 0.89 \pm 0.04$ and $\sigma_{1,3\text{-dimethylurea}} = 0.98 \pm 0.05$, each the average of two experiments disagree with our present values. They were determined by the same method as the present values, which are the averages of a greater number of experiments, and we cannot account for the difference.

The urea permeability coefficient is given in a variety of units. Since our $K_{m,urea}$ (Table II) $= 0.3 \pm 0.07$ molal, our $J_{max,urea} = (4.3 \pm 1.7) \cdot 10^{-7}$ molcm^{-2}s^{-1}, in fair agreement with Brahm's [25] value of $1.3 \cdot 10^{-7}$ molcm^{-2}s^{-1}, but much better agreement with Yousef and Macey's [15] figure of $(3.1 \pm 0.5) \cdot 10^{-7}$ molcm^{-2}s^{-1}. We agree less well with Karan and Macey's recent value of $1.14 \cdot 10^{-7}$ molcm^{-2}s^{-1} for J_{max}. Mayrand and Levitt [13] give $P_o = 1.2 \cdot 10^{-3}$ cms^{-1} at zero trans urea concentration ($= J_{max}/K_m$) which is in very good agreement with our value of $J_{max}/K_m = (1.4 \pm 0.6) \cdot 10^{-3}$ cms^{-1}. The most surprising disagreement is with the recent determinations of Macey's group [14,26] of $K_{m,urea} = 680$ mM since that figure lies well out along the plateau of our urea single site binding curve in Fig. 5.

In the case of methylurea, our $\omega_{methylurea}$ is equivalent to $P_{d,methylurea} = 3.2 \cdot 10^{-5}$ cms^{-1} at 180 mmolal methylurea, which agrees well with Yousef and Macey's [15] $P_o = 3.2 \cdot 10^{-5}$ cms^{-1} at 277 mM methylurea. Our results for 1,3-dimethylurea do not agree with Yousef and Macey [15] who found that the permeability of 1,3-dimethylurea follows simple diffusion, while we observe the permeability to saturate with $K_m = 0.23 \pm 0.06$ molal.

TABLE II

Permeability coefficients for amides and ureas

	K_m (molal)	ω_i (10^{-15} mol dyn^{-1} s^{-1})	P_d (10^{-4} cm s^{-1})
Formamide	0.40 ± 0.08 (4)	28.9 ± 9.0	7.05 ± 2.2
N-Methylformamide	0.43 ± 0.15 (4)	26.0 ± 8.7	6.34 ± 2.1
Acetamide	0.37 ± 0.15 (3)	11.3 ± 2.2	2.76 ± 0.5
N-Methylacetamide	0.55 ± 0.17 (4)	5.9 ± 1.1	1.44 ± 0.3
Propionamide	0.35 ± 0.14 (7)	6.7 ± 1.6	1.63 ± 0.4
Urea	0.30 ± 0.07 (7)	29.5 ± 7.6	7.20 ± 1.9
Methylurea	0.09 ± 0.04 (4)	7.6 ± 2.4	1.85 ± 0.6
Ethylurea	0.47 ± 0.31 (3)	0.9 ± 0.3	0.22 ± 0.07
1,3-Dimethylurea	0.23 ± 0.06 (4)	2.4 ± 0.2	0.59 ± 0.05
1,1-Dimethylurea	0.33 ± 0.16 (4)	1.4 ± 0.3	0.34 ± 0.07

significant feature of amide and urea permeation *. The values of K_m given in Table II fall in a broad band centered around 400 mM, with the values for the ureas at the lower end of the spectrum, and with one solute, methylurea ($K_m = 90 \pm 40$ mM), bound tighter than the others. Our present values of ω_i given in Table II (which also contains the P_d values derived from them) can not be compared directly with the previous ones determined by Sha'afi et al. [24] because the red cell area has been determined more accurately in the intervening decades (present value $1.35 \cdot 10^{-6}$ cm^2 (see Jay [8]); previous value, $1.67 \cdot 10^{-6}$ cm^2). To express the previous values in terms of the present area, they have to be multiplied by a factor of 1.6, as described by Toon and Solomon [2]. With this correction, the values are in reasonable agreement, as shown in the footnote on p. 185, an agreement which is somewhat unexpected because we did not know about the concentration dependence of these ω_i values in 1971.

* Staffero and Yousef [30] and Yousef (private communication) reported that, in addition to the saturable component, there was a large linear component in acetamide flux across the human red cell membrane at pH 6.0. At this pH, $J_{max,acet}$ was $1.1 \cdot 10^{-7}$ mol cm^{-2} s^{-1}, about 60% of the $J_{max,acet}$ that we observed at pH 7.4. We carried out six experiments with acetamide and found clear evidence for a saturable site with no linear component (as analysed by non-linear least squares) in three experiments, whose results are averaged in Table II. In the other three experiments, there was a large linear component and we don't understand why. Staffero and Yousef suggest that the linear component should be ascribed to lipid permeation but we think this is unlikely for two reasons. First, the apparent activation energy for acetamide permeation determined by Galey et al. [31] was 12 ± 2 kcal mol^{-1}, typical of permeation through an aqueous channel, as compared to values of 26 to 48 kcal mol^{-1} for butyramide and valeramide which are believed to permeate through the lipid. Second, there was no evidence for a linear component of permeability in our measurements of the permeation of other amides, either for formamide or for *N*-methylacetamide and propionamide, whose additional -CH_2 group would enhance lipid solubility.

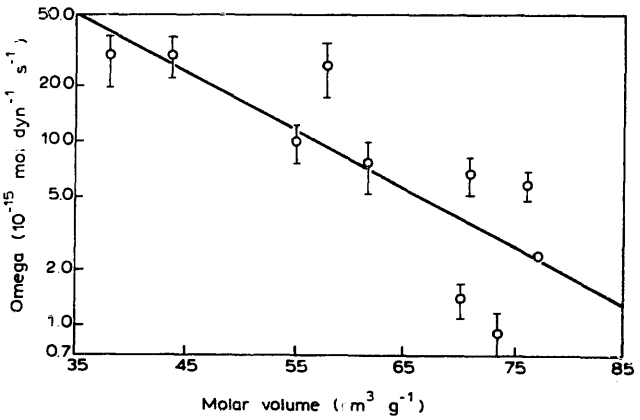

Fig. 6. Linear correlation of ln ω_i with molar volume ($r = 0.81$; $P < 0.01$, *t*-test).

The importance of molar volume as a determinant of permeation is illustrated in Fig. 6 which shows that ln ω_i is linearly and significantly ($P < 0.01$, *t*-test; $r = 0.81$) correlated with $\bar{V}_s$, consistent with expectations based on diffusion through a sieve-specific channel. The importance of solute diameter is shown by comparing 1,3-dimethylurea (diameter = 5.24 Å) with 1,1-dimethylurea (diameter = 5.64 Å) and observing that the bulky configuration of the two methyl groups on the 1,1 compound reduces ω_i from $(2.4 \pm 0.2) \cdot 10^{-15}$ mol dyn^{-1} s^{-1} to $(1.4 \pm 0.3) \cdot 10^{-15}$ mol dyn^{-1} s^{-1}.

Since both ω_i and $f(\sigma_i)$ are correlated with solute dimensions, it is to be expected that they will be correlated with one another and Fig. 7 shows that $f(\sigma_i)$ is linearly dependent on ω_i ($P < 0.01$, *t*-test; $r = 0.8$). These three correlations mean that molecular dimensions modulate both ω_i and σ_i, which is to be expected as a natural consequence of the friction within the sieve-specific aqueous channel. Though it is possible that a specialized transport protein, as put forward by Wieth et al. [14] and subsequently many other investigators [13,17,32–34], could regulate the passage of urea

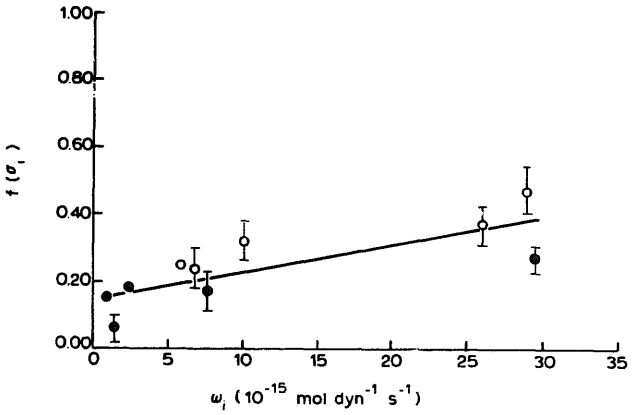

Fig. 7. Dependence of $f(\sigma_i)$ on ω_i. The urea family of solutes is denoted by the filled circles. The data have been fitted to a straight line with intercept, 0.15 ± 0.04 and slope = $(8 \pm 2) \cdot 10^{12}$ dyn s mol^{-1} by least squares. ($r = 0.8$; $P < 0.01$, *t*-test).

and the amides strictly according to molecular size, this is hardly to be expected. Furthermore, it is not possible to see how the transport protein could also provide the correlated effect on $f(\sigma_i)$ shown in Fig. 4. These considerations lead to the conclusion that the correlations in Figs. 4, 6 and 7 provide very strong evidence that urea and the amides cross the red cell membrane through an aqueous channel in which solute/membrane friction is a dominant factor *.

Hydrogen bonds and problems of lipid solubility

We carried out a series of experiments on the amides to see whether we could illustrate the effect of H-bonds on amide permeability, similar to those we had found in the alkanol series. For this purpose, we chose two pairs of compounds: *N*-methylformamide vs. acetamide and *N*-methylacetamide vs. propionamide. The members of each pair contain the same number of $-CH_2$ groups, but differ by one putative hydrogen bond. Unfortunately, geometric considerations vitiated both comparisons. The additional H-bonding capacity in acetamide as compared to *N*-methylformamide does indeed decrease ω_i from $26.0 \cdot 10^{-15}$ to $10.0 \cdot 10^{-15}$ mol dyn^{-1} s^{-1}, but it also increases the diameter from 4.68 to 5.24 Å, so that we cannot deconvolute the causes. Similarly, there is no difference in ω_i between *N*-methylacetamide and propionamide, ω_i changing only from $5.9 \cdot 10^{-15}$ to $6.7 \cdot 10^{-15}$ mol dyn^{-1} s^{-1}, while the diameter decreases from 5.32 to 5.20 Å.

In a further attempt to obtain information about H-bonding in the amide series, we studied one additional pair of solutes, *N*-methylpropionamide and *N*-ethylacetamide, which have three methyl groups, one more than any of the amides in Tables I and II. These larger amides differ from one another only in the placement of one $-CH_2$ group since both have the same number of H-bonds. Far from throwing additional light on the properties of the other amides, these two solutes behaved aberrantly, because the additional $-CH_2$ group is sufficient to cause an important increase in lipid solubility, as can be shown from the apparent activation energies. Galey et al. [31] showed that the apparent activation energy for permeation of the red cell membrane by small hydrophilic solutes such as urea, formamide and acetamide was 11–12 kcal mol^{-1}. Addition of one $-CH_2$ group to propionamide increased the apparent activation energy to 19 ± 3 kcal mol^{-1} and a second $-CH_2$ group increased the apparent activation energy still further to 26 ± 2 kcal mol^{-1} for butyramide, consistent with permeation through the lipids. Diamond and Wright [36] have shown that the free energy terms for the lipid : water partition coefficient of specific groups are essentially additive so that, to a first approximation, any molecule comprising three methyl groups and an amide has the same lipid solubility. Replacement of one putative amide H-bond by a methyl group in *N*-ethylacetamide and *N*-methylpropionamide means that their solubility in the red cell membrane lipids would be greater than that of butyramide. In view of these considerations membrane solubility must be included explicitly in the analysis of the flux of these two solutes.

In their original article on the application of irreversible thermodynamics to membrane permeability, Kedem and Katchalsky [37] showed that the reflection coefficient for a solute that could only permeate the membrane by dissolution was given by:

$$\sigma_i = 1 - (\omega_i \bar{V}_s / L_p) \tag{8}$$

which validates the use of the $\omega_i \bar{V}_s / L_p$ term to specify the contribution of permeation through the membrane. Dainty and Ginzburg [38] have given a general solution to the Kedem and Katchalsky equations which explicitly includes separate terms for passage through the channels and passage through the membrane. Their general solution appears intractable, but they have provided simplified approximations which reduce to Eqn. 8, for every case which they consider, including the one in which solute permeates by both routes and the solvent passes only through aqueous channels. The Dainty and Ginzburg treatment provides a theoretical basis for Eqn. 6 which we have used in computing Tables I and II and which leads to a consistent body of data but, as we shall see, its validity is limited to hydrophilic solutes.

We have determined σ_i for the two lipophilic solutes and obtained the values given in Table III, 0.55 for *N*-ethylacetamide and 0.43 for *N*-methylpropionamide, much lower than those for the next lower members of the series, with $\sigma_i = 0.72$ for both *N*-methylacetamide and propionamide. Ideally, the mathematical apparatus of Dainty and Ginzburg [38] should provide a correc-

* Zanner et al. [35] have concluded that urea and water do not traverse the same aqueous channel on the basis of water and urea permeability changes induced in malaria-infected human red cells. They report that malaria infection causes a 62% decrease in the osmotic permeability coefficient, P_f, a concomitant average 41% increase in the diffusional permeability coefficient, P_d and no change in the urea permeability coefficient. The change in P_f means that: either the number of pores remains constant and their diameter decreases, or that the diameter remains constant and the number of pores decreases. In either case, P_d, which is a measure of the total membrane area available for water diffusion, must also decrease. Since P_d is observed to increase, malaria infection must cause new channels to open, whose characterization with respect to water and urea transport is unknown. Thus, no valid inferences about the water and urea permeability characteristics of the normal cell may be drawn from the behavior of an infected cell. The observed constancy of the urea fluxes presumably reflects some mixture of the properties of the original channels and the malaria induced ones and may well be related to the accelerated uptake of exogenous amino acids that has been observed in malaria-infected cells.

TABLE III

Reflection and permeability coefficients for lipid-soluble amides

	N-Ethyl-acetamide	*N*-Methyl-propionamide	Unit
diameter	5.32	5.32	Å
$\bar{V}$	92.5	93.6	$cm^3\,mol^{-1}$
$\omega\bar{V}/L_p$	0.085	0.157	
σ_i	0.55	0.43	
$f(\sigma_i)$	0.365	0.413	
Apparent K_m	0.47	0.58	molal
Apparent ω_i	11.7	21.5	10^{-15} $mol\,dyn^{-1}\,s^{-1}$

tion, with very large values of $\omega_i\bar{V}_s/L_p$ to bring $f(\sigma_i)$ in line with the other amides so that $f(\sigma_i)$ would approximate the fitted line in Fig. 7 with values of approx. 0.24 for *N*-ethylacetamide and approx. 0.32 for *N*-methylpropionamide, rather than the values of 0.365 and 0.413, given in Table III. This disagreement calls into question the approximations used in the simplification of Dainty and Ginzburg [38]. Unfortunately, we have not been able to make a critical examination of their arguments because the simplification has been done by inspection and the inspection has eluded us. Since, as far as we know, there have not been previous investigations in which all three phenomenological coefficients have been measured for flux across a single plasma membrane, it has not previously been possible to put the Dainty and Ginzburg equations to experimental test. Our results, however, lead us to believe that their treatment does not provide an adequate description of flux across the red cell membrane when there is a significant lipophilic contribution.

Permeation of both *N*-ethylacetamide and *N*-methylpropionamide is a saturable process with apparent K_m values of 0.47 and 0.58 molal as given in Table III. The curves are similar to that for urea in Fig. 5, but the flux continues to rise even at the highest solute concentrations that we used, which we ascribe to the linear term for membrane dissolution which must be added to the saturable term for passage through the channel. The fact that there is a clearly defined K_m for both solutes means that there is a significant contribution from channel passage, but we did not go out to high enough solute concentrations to determine the linear term. We have computed the apparent ω_i in Table III by the same convention used for the other solutes. The apparent ω_i values of $11.7 \cdot 10^{-15}$ and $21.5 \cdot 10^{-15}$ $mol\,dyn^{-1}\,s^{-1}$ for *N*-ethylacetamide and *N*-methylpropionamide, respectively, are reasonably close to the maximum fluxes from the fitted curves of $9.4 \cdot 10^{-15}$ and $20 \cdot 10^{-15}$ $mol^2\,dyn^{-1}\,cm^{-3}\,s^{-1}$, which are reached at 3–4-times the K_m, so that the apparent ω_i values are reasonable approximations to the permeability coefficients at high solute concentrations.

Conclusion

The permeation of all the ureas and amides we have studied is a saturable process which fits a single site binding curve and does not follow simple diffusion kinetics. According to our model of the red cell pore, the first step in membrane transport is binding to an H-bond exchange site where urea and the amides exchange their solvation shell with membrane H-bonds, as required for entrance into the sieve-specific channel which traverses the membrane. We have found that the corrected reflection coefficient, $f(\sigma_i)$, is significantly less than zero for nine ureas and amides, which provides very strong thermodynamic evidence that these molecules enter the red cell through an aqueous pore.

Inside the sieve-specific channel, the solute is subject to frictional forces with the membrane, whose existence is shown by our observation that ω_i is linearly dependent upon solute molar volume. Since $f(\sigma_i)$ is linearly correlated both with solute diameter and ω_i, there is a common element, solute volume, which modulates both parameters. If, as has been frequently suggested, there were a specialized protein in the red cell membrane that transports urea, but not water, it is difficult to understand why nature would have gone to such pains to regulate the transport according to molecular size when it could have achieved the same ends so much more easily with a simple aqueous pore.

Appendix

Our evidence shows that water and small nonelectrolytes permeate the membrane through an aqueous pore. If this is so, there is a thermodynamic requirement for solvent drag and yet Brahm and Galey [22] have concluded that there is no solvent drag on urea flux across the human red cell membrane. In view of this direct conflict, we have made a critical examination of the

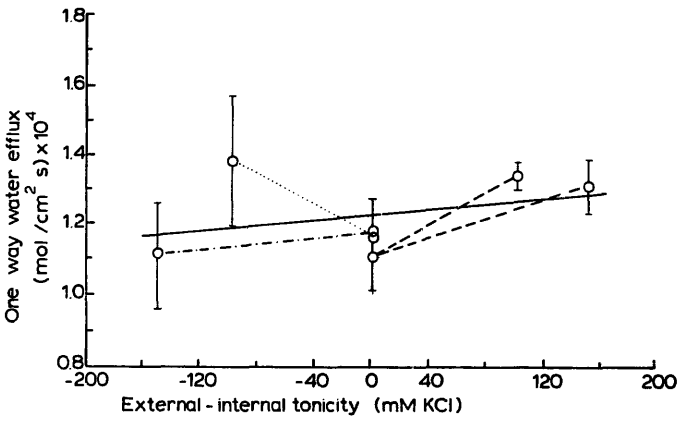

Fig. A-1. Net water efflux as a function of osmotic pressure gradient, from the data of Brahm and Galey [22]. The connecting lines are coded to the initial KCl concentration (- - - - -, 100 mM; · · · · · ·, 150 mM; –·–·–·–, 200 mM).

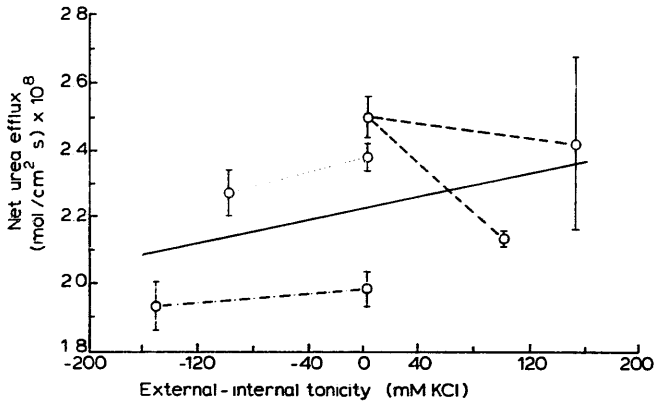

Fig. A-2. Net urea efflux as a function of osmotic pressure gradient, from the data of Brahm and Galey [22].

statistical basis of the Brahm and Galey conclusion. They first carried out experiments to show that osmotic water flux caused solvent drag in tracer water flux and we have plotted the data from their Table IIIA in Fig. A-1 to see whether there is a linear relationship between the observed tracer water efflux and the applied osmotic pressure as theory requires and as Andersen and Ussing [23] showed to be the case in the isolated toad skin. Brahm and Galey carried out paired experiments at three different ambient osmolalities and the pairs at each osmolality are connected in Fig. A-1. Brahm and Galey give figures for the maximum and minimum values at each point and we have set half the length of our error bars equal to half the excursion. The least-squares fitted line has a slope of $(4 \pm 4.6) \cdot 10^{-5}$ $cm^{-2} s^{-1}$ and an intercept of $(1.27 \pm 0.04) \cdot 10^{-4}$ $mol\,cm^{-2} s^{-1}$. The apparent linear dependence of tracer water efflux on osmotic gradient * is not statistically significant since $r = 0.36$ and the t-test of significance gives $P > 0.1$. This is not surprising since the flux goes against the osmotic pressure gradient in one of the four paired sets of data.

Fig. A-2 shows a similar plot for the urea data at 38°C where the bulk of the measurements were made (their Table V). In this case, the least squares fitted line has a slope of $(9.2 \pm 8.6) \cdot 10^{-9}$ $cm^{-2} s^{-1}$ and an intercept of $(2.2 \pm 0.1) \cdot 10^{-8}$ $mol\,cm^{-2} s^{-1}$, but the apparent linearity is again not significant because $r = 0.43$ and $P > 0.1$. In the urea case, the control data at zero osmotic gradient, as Galey and Brahm point out, clearly depend upon the ambient osmolality and the fit of the least-squares line is not an acceptable criterion. Nonetheless, the dependence of urea flux on the osmotic pressure gradient is clouded since two of the fluxes go with the osmotic pressure gradient and two against.

* For clarity, we take the sense of the osmotic pressure gradient to be (higher–lower) so solvent moves with the osmotic pressure gradient, that is rightward in Figs. A-1 and A-2.

Fortunately, there is another statistical criterion which is free of the constraints of the least squares regression line. This is the equivalent slope of the line connecting each pair of coupled flux measurements in Fig. A-1, taken in the sense of the right terminus divided by the left terminus normalized to an osmotic pressure gradient of 100 mM KCl. In order to make an unequivocal demonstration of a solvent drag effect on water efflux, $(\text{equiv slope})_{water}$ must be greater than 1.0. In fact, the average $(\text{equiv slope})_{water}$ is 1.056 ± 0.161. Using the t-test to determine whether this slope is significantly greater than 1.0, $P > 0.5$. This means that there is no statistical basis for concluding that the Brahm and Galey experiments show that osmotic pressure gradients exercise solvent drag on tracer water efflux.

The next step is to determine whether there is any different effect on the tracer flux for urea. In statistical terms, the question is: is $(\text{equiv slope})_{water} - (\text{equiv slope})_{urea} > 0$? The $(\text{equiv slope})_{urea}$ is 0.974 ± 0.086. The t-test shows that the probability that the difference between these two slopes is greater than 0 is $P > 0.5$. Therefore there is no statistically significant difference between the effect of applied osmotic pressure gradients on the flux of tracer water and that of tracer urea.

Acknowledgments

This study was supported in part by The Council for Tobacco Research - U.S.A., Inc. and by the Squibb Institute for Medical Research.

References

1 Katchalsky, A. and Curran, P.F. (1965) Nonequilibrium Thermodynamics in Biophysics, Harvard University Press, Cambridge, MA.
2 Toon, M.R. and Solomon, A.K. (1990) Biochim. Biophys. Acta 1022, 57–71.
3 Terwilliger, T.C. and Solomon, A.K. (1981) J. Gen. Physiol. 77, 549–570.
4 Goldstein, D.A. and Solomon, A.K. (1960) J. Gen. Physiol. 44, 1–17.
5 Chasan, B. and Solomon, A.K. (1985) Biochim. Biophys. Acta 821, 56–62.
6 Toon, M.R. and Solomon, A.K. (1987) Biochim. Biophys. Acta 898, 275–282.
7 Sha'afi, R.I., Rich, G.T., Mikulecky, D.C. and Solomon, A.K. (1970) J. Gen. Physiol. 55, 427–450.
8 Jay, A.W.L. (1975) Biophys. J. 15, 205–222.
9 Savitz, D., Sidel, V.W. and Solomon, A.K. (1964) J. Gen. Physiol. 48, 79–91.
10 Solomon, A.K., Toon, M.R. and Dix, J.A. (1986) J. Membr. Biol. 91, 259–273.
11 Levin, S.W., Levin, R.L. and Solomon, A.K. (1980) J. Biochem. Biophys. Methods 3, 255–272.
12 Solomon, A.K. (1989) Methods Enzymol. 173, 192–222.
13 Mayrand, R.R. and Levitt, D.G. (1983) J. Gen. Physiol. 81, 221–237.

14 Wieth, J.O., Funder, J., Gunn, R.B. and Brahm, J. (1974) in Comparative Biochemistry and Physiology of Transport (Bolis, L., Block, K., Luria, S.E. and Lynen, F., eds.), pp. 317–337, North Holland, Amsterdam.
15 Yousef, L.W. and Macey, R.I. (1989) Biochim. Biophys. Acta 984, 281–288.
16 Toon, M.R. and Solomon, A.K. (1987) J. Membr. Biol. 99, 157–164.
17 Levitt, D.G. and Mlekoday, H.J. (1983) J. Gen. Physiol. 81, 239–253.
18 Solomon, A.K. and Chasan, B. (1980) Fed. Proc. 39, 957a.
19 Toyoshima, C. and Unwin, N. (1988) Nature 336, 247–250.
20 Edwards-Moulds, J. and Kasschau, M.R. (1988) Vox Sang. 55, 181–185.
21 Fröhlich, O., Gunn, R.B., Gargus, J.J. and Rizzolo, L.J. (1988) Biophys. J. 53, 531a.
22 Brahm, J. and Galey, W.R. (1987) J. Gen. Physiol. 89, 703–716.
23 Andersen, B. and Ussing, H.H. (1957) Acta Physiol. Scand. 39, 228–239.
24 Sha'afi, R.I., Gary-Bobo, C.M. and Solomon, A.K. (1971) J. Gen. Physiol. 58, 238–258.
25 Brahm, J. (1983) J. Gen. Physiol. 82, 1–23.
26 Karan, D.M. and Macey, R.I. (1990) Biochim. Biophys. Acta 1024, 271–277.
27 Renkin, E.M. (1954) J. Gen. Physiol. 38, 225–243.
28 Giebel, O. and Passow, H. (1960) Pflugers Arch. 271, 378–388.
29 Soll, A.H. (1967) J. Gen. Physiol. 50, 2565–2578.
30 Staffero, L. and Yousef, L.W. (1990) Biophys. J. 57, 91a.
31 Galey, W.R., Owen, J.D. and Solomon, A.K. (1973) J. Gen. Physiol. 61, 727–746.
32 Brahm, J. and Wieth, J.O. (1977) J. Physiol. 266, 727–749.
33 Macey, R.I. (1984) Am. J. Physiol. 246, C195–C203.
34 Fröhlich, O. and Jones, S.C. (1988) Biochim. Biophys. Acta 943, 531–534.
35 Zanner, M.A., Galey, W.R., Scaletti, J.V., Brahm, J., Vander Jagt, D.L. (1990) Mol. Biochem. Parasitol. 40, 269–278.
36 Diamond, J.M. and Wright, E.M. (1969) Annu. Rev. Physiol. 31, 581–646.
37 Kedem, O. and Katchalsky, A. (1958) Biochim. Biophys. Acta 27, 229–246.
38 Dainty, J. and Ginzburg, B.Z. (1963) J. Theoret. Biol. 5, 256–265.